Notes

Fine Structures in Phase-Separated Domains of a Polyolefin Blend via Spinodal Decomposition

Xiaohua Zhang,† Zhigang Wang,‡ and Charles C. Han*,†

Beijing National Laboratory for Molecular Sciences, Joint Laboratory of Polymer Science and Materials, State Key Laboratory of Polymer Physics and Chemistry, CAS Key Laboratory of Engineering Plastics, Institute of Chemistry, Chinese Academy of Sciences, Beijing 100080, China

Received May 11, 2006
Revised Manuscript Received July 19, 2006

Introduction

Polyethylene (PE) is one of the mostly used and common polymeric materials. To improve its properties, it is often blended with other polymers, such as elastomers of random olefin copolymers. It is very important to understand the fundamental physics of mixing these polymers in order to control the final properties through the specific compounding and manufacturing processes. In the case of linear low-density polyethylene (LLDPE) blends, the mixtures can undergo both liquid−liquid phase separation (LLPS) and crystallization. These processes affect greatly the morphology and properties of the final products. Both phase separation phenomena[1−4] and crystallization kinetics[5,6] have been studied extensively in polyolefin blends. However, only limited studies have been reported on the simultaneous phase separation and crystallization processes.[7−14] The dynamics of spinodal decomposition (SD) and the pattern formation of polymer blends have been the subjects of both theoretical and experimental investigations and provide fascinating examples of nonlinear nonequilibrium phenomena.[15−17] Over the past two decades, many studies have been made to investigate the growth of concentration fluctuations via SD employing light scattering[18−20] and neutron scattering[21−23] measurements. The characteristic morphology of the SD process, bicontinuous and interconnected tubelike structure, and its growth have been well studied and are reasonably well understood, at least from a global and statistical point of view. By the double-quench experiment[24−27] or other techniques,[28−30] the dotlike small objects inside phase-separated domains can be studied. On the other hand, the fine structures in the "late-stage" SD process and crystallization remain largely unexplored. Thus, two-step phase separation was here introduced by double temperature quench to obtain the crystallized fine structures inside phase-separated domains. In the "late stage" of the SD process, the bicontinuous structures may break up and grow into larger objects,[31] and subsequent crystallization or phase separation/crystallization process could generate a unique morphology with both fundamental and applicational importance and interest. In the present report we studied the fine structures in the "late-stage" SD process. We investigated the mechanism of the formation of the fine structures and identified the observed morphologies formed through a multistep phase separation/crystallization process.

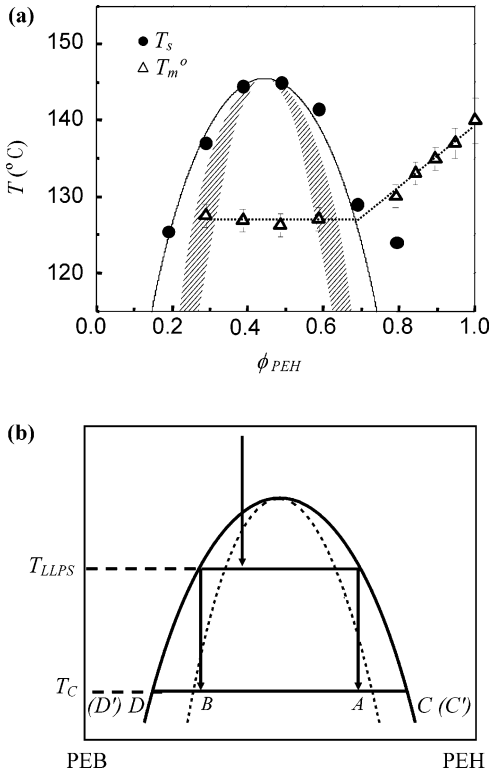

Figure 1. (a) Phase diagram of PEH/PEB blends.[14] The symbols (filled circles) correspond to experimental data points of the binodal temperature (T_S) and the solid line to the fit of the Flory−Huggins theory. The additional symbols (open triangles) display the equilibrium melting points of the indicated blends. (b) Schematic diagram of the "second-step" phase separation. *A* denotes originally PEH-rich domain, *B* originally PEB-rich domain, *C* PEH-rich domain in *A* after second quench, *C*′ PEH-rich domain in *B* after second quench which can only be observed after 20 h of LLPS, *D* PEB-rich domain in *A* after second quench, and *D*′ PEB-rich domain in *B* after second quench.

Experimental Section

Materials. The materials are statistical copolymers of ethylene/hexene (PEH) (M_w = 110 kg/mol, 2 mol % hexene comonomer) and ethylene/butene (PEB) (M_w = 70 kg/mol, 15 mol % butene comonomer). They were supplied by ExxonMobil Co. Ltd., synthesized with metallocene catalysts, and have relatively narrow molecular weight polydispersities (∼2) and relatively uniform comonomer distributions.[14] PEH is the only crystallizable component of this blend system above 60 °C. PEB can crystallize below 60 °C (see Supporting Information), while the crystals cannot be observed by AFM and polarized optical microscopy. The crystallization peak is very small and weak. In the room temperature, the PEB is a transparent elastomer. Therefore, it is concluded that the PEB chains only form microcrystal and the crystallinity is very

* To whom correspondence should be addressed: e-mail c.c.han@iccas.ac.cn; Tel +86-10-82618089; Fax +86-10-62521519.
† State Key Laboratory of Polymer Physics and Chemistry.
‡ CAS Key Laboratory of Engineering Plastics.

10.1021/ma061064i CCC: $33.50
Published on Web 09/23/2006

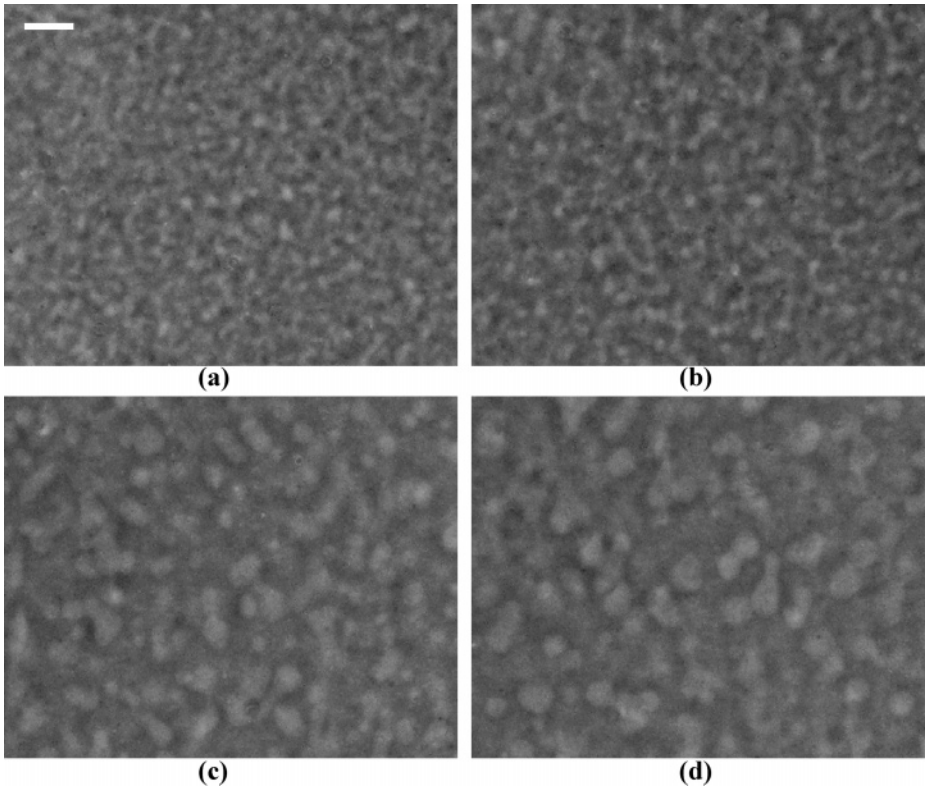

Figure 2. Phase contrast optical micrographs of LLPS at 135 °C for (a) 6, (b) 10, (c) 12, and (d) 20 h. The scale bar in (a) corresponds to 10 μm and is applied to (b)−(d).

low. The blend of PEH and PEB which has a PEH mass fraction of 30% was prepared by the coprecipitation method. PEH and PEB with mass ratio of 30 to 70 were first dissolved in hot xylene at 120 °C, and then the solution was cooled to 100 °C and kept for 24 h. The solution was then poured into a cool methanol (0 °C) bath to precipitate the blend. After filtration, the obtained blend was further washed with methanol and then dried in a vacuum oven for 72 h before use.

Sample Preparation and Characterization by OM and AFM. The samples of the blend were hot-pressed at 160 ± 2 °C to form films of ca. 20 μm (for OM) and then quenched to room temperature.

The phase contrast optical microscopy (PCOM) observation was carried out by using an Olympus (BX51) optical microscope and an Olympus (C-5050ZOOM) camera. The polarized optical microscopy (POM) observation was carried out by using a Nikon (L-UEPI) optical microscope with a Nikon (COOLPIX4500) camera. A hot stage (Linkam, LTS350) was used to control the sample temperature.

AFM images were obtained by using a NanoScope III MultiMode AFM (Digital Instruments). Silicon cantilever tips with a resonance frequency of ∼300 kHz and a spring constant of ∼40 N/m were used. The scan rate ranged from 0.5 to 1.5 Hz/s. The sample line was 512, and the target amplitude was 2 V. Height and phase images were recorded simultaneously during scanning. The films of the blend (ca. 20 μm) were prepared by hot-pressing at 160 ± 2 °C onto silicon wafer surfaces (10 mm × 10 mm) by using two pieces of silicon wafer. After cooling to room temperature the cover silicon wafer was removed to ensure the film surface examination by AFM. Before further annealing at the temperature of LLPS, the samples are heated to homogenization temperature of 160 °C for 10 min to ensure the erasing of the influence of the Si wafer on top of the sample and thermal history before they were rapidly cooled to the desired LLPS temperature. The thickness of the samples used for the AFM measurement is about 20 μm, which can be considered as bulk sample. Therefore, the interfacial effect is small or negligible. For AFM measurement, first the PEH-rich and PEB-rich domains are chosen by using the optical microscope equipped in the AFM, and then the AFM scanning proceeds in each chosen domain in order to observe crystallized structures inside PEB-rich and PEH-rich domains. The phase contrast AFM is used to locate the crystals. The AFM phase contrast is based on a difference in "surface hardness" of the crystal vs the amorphous component. Because the modulus difference between the crystals and amorphous component is large, AFM phase images provide better contrast for revealing the crystalline and amorphous morphology of blends.

Results and Discussion

Interconnected Bicontinuous Structures Observed by PCOM. The phase diagram of PEH/PEB blends shown in Figure 1a was determined and reported previously.[14] The microscopy is helpful to derive phase diagrams for these kinds of blends.[32] The phase diagram exhibits an upper critical solution temperature (UCST) with critical point located at the temperature of 146 °C and at the composition of 0.44. Also shown in the phase diagram are the equilibrium melting temperatures of the blends determined previously by using the Hoffman−Weeks extrapolation method.[14] For the miscible polymer blends, the equilibrium melting temperature depends on the PEH volume fraction, which depresses with decreasing of PEH concentration. For phase-separated blends, after long time LLPS, the two phase-separated phases reach their equilibrium coexistence compositions. Therefore, for all phase-separated blends, their equilibrium coexistence compositions are the same and so are the equilibrium melting temperatures.

On the basis of the information provided in Figure 1a and in ref 14, the PEH/PEB = 30/70 blend is within the two-phase region of the phase diagram at 135 °C. Figure 2 shows the phase contrast optical micrographs of PEH/PEB = 30/70 blend at the LLPS temperature of 135 °C for different annealing time. Phase separation in the original homogeneous blend can be observed after annealing for 220 min. Beyond the 6 h annealing time, the bicontinuous and interconnected tubelike structure grows

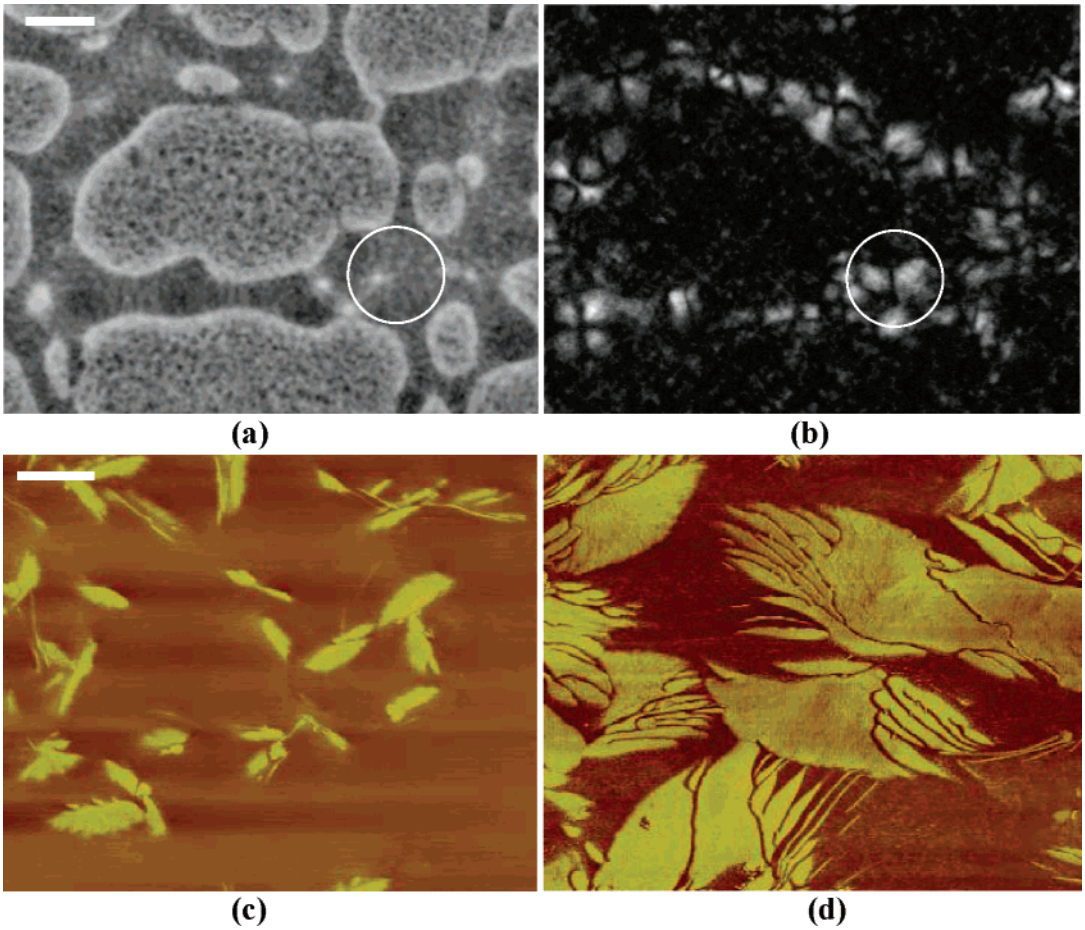

Figure 3. (a) Phase contrast optical micrograph, (b) polarized optical micrograph, (c) atomic force micrograph in the PEB-rich domain, and (d) atomic force micrograph in the PEH-rich domain of the PEH/PEB = 30/70 blend at room temperature after LLPS at 135 °C for 20 h. The scale bar in (a) corresponds to 10 μm and is applied to (b); the scale bar in (c) corresponds to 500 nm and is applied to (d).

and coarsens with the annealing time, as shown in Figure 2. This bicontinuous structure signifies the typical spinodal decomposition of LLPS. When staying at 135 °C for more than 12 h, the bicontinuous structures start to break up and merge into macrospheres.[33] These characteristics agree with the late stage coarsening prediction of the spinodal decomposition mechanism.

Phase Separation within the Phase-Separated Domains. Because of irregularity of the broken-up or merged domain structures, large macrospheres were chosen for the detailed observation after the sample was cooled to room temperature (see Figure 3). By this double-quench procedure,[25−27] the dotlike small objects inside phase-separated domains can be studied. The phase-separated domains shown in Figure 3a,b were captured by using the phase contrast and polarized optical microscopy at the same location of the PEH/PEB = 30/70 blend. Figure 3a clearly shows that the bicontinuous structures break up or grow into large objects after LLPS at 135 °C for 20 h. By comparing with that in Figure 3b, we can conclude that the dark part (circled part) in Figure 3a corresponds to the light part (circled part) in Figure 3b, which is the PEH-rich domain, and the light part in Figure 3a corresponds to the dark part in Figure 3b, which is the PEB-rich domain. The contrast in phase contrast and polarized optical micrographs shown in Figure 3 is associated with the difference of refractive indices between the two components[34] (Figure 3a) and with the different crystalline structures (Figure 3b), respectively. If the PEB-rich domains were homogeneous, they should have appeared light under PCOM observation and dark under POM observation. However, with a more detailed observation of Figure 3, we can find that the PEB-rich domains do not appear to be homogeneous; instead, they consist of dotlike small objects. The small objects have characteristic sizes of less than 1 μm. This result suggests that the PEB-rich domains contain inhomogeneity in refractive index at the submicrometer scale. By using AFM, we can further look into the domains at small scales. Figure 3c shows that short and small lamellae can be formed in the PEB-rich domains. The lamellae in PEB-rich domains look more isolated and imperfect than those in PEH-rich domains (Figure 3d). This suggests that an additional phase separation could occur in the PEB-rich domains, in which PEH could form lamellae when the blend is cooled to room temperature. The formation of such more imperfect lamellar crystals also suggests that PEH in the PEB-rich domains may contain higher branching contents, which is consistent with the fact that PEH with higher α-monomer content has better miscibility with PEB than PEH with more linear chains.[1,35−38] The observed morphology consists of phase-separated and crystallized domains within phase-separated domains. When crystallization happens at low temperature, the second-step morphology evolution takes place. That means the second step of structure formation is induced by the crystallization. The crystallization temperature/degree of undercooling is the driving force of crystallization. The second phase separation is driven by the crystallization. However, we cannot rule out the possibility that due to the lower PEH concentration in PEB-rich domains, the PEH crystal growth may be interfered by the presence of PEB chains, and consequently more isolated and imperfect PEH crystals are produced. For a

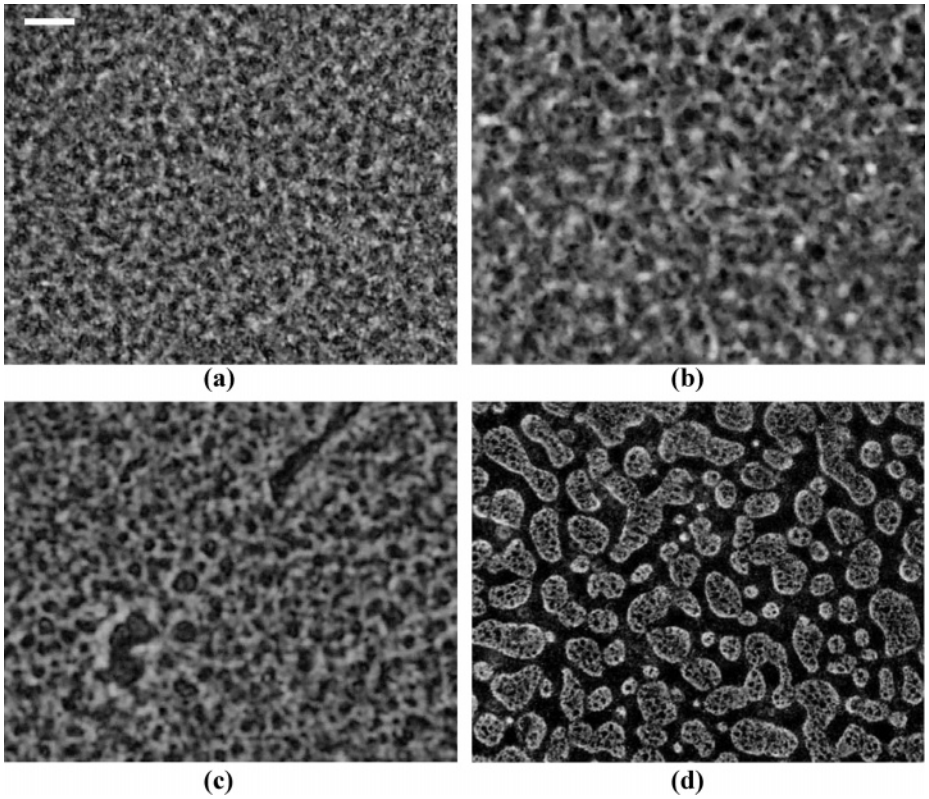

Figure 4. Phase contrast optical micrographs of the PEH/PEB = 30/70 blend at room temperature after LLPS at 135 °C for (a) 6, (b) 10, (c) 12, and (d) 20 h. The scale bar in (a) corresponds to 10 μm and is applied to (b)−(d).

relatively short time of LLPS, the characteristic length for phase separation is small, and because of the higher PEH concentration inside the PEB-rich domains compared with the case of long LLPS time, the crystals in the PEH-rich domain could grow toward the PEB-rich domain by absorbing the PEH chains at the boundary. While in the PEB-rich domain near the boundary, where the PEH concentration is relatively high compared with the center part of PEB-rich domain, crystallization is coupled with the exclusion of the amorphous PEH chains and PEB chains. PEH sequences at the boundary and in the PEB-rich domain near the boundary that can be oriented with the right conformation and incorporated into the crystals may be separated from those sequences near entanglements and with more branches that cannot crystallize and can only be part of the amorphous regions. But the crystal could not grow through the PEB-rich domain and enter into the next PEH domain. In the growth front, the depleted region was formed. The high barrier of the depleted region due to composition inhomogeneity prohibits spherulites from growing further. Another possibility is that the newly formed small crystals in the PEB-rich domain may break up the boundaries of the PEB-rich domain and contact with the large crystals in PEH-rich domains. Therefore, the fine structures cannot be observed in the case of short LLPS time.

Evolution of Phase-Separated Domains. Figure 4 shows the phase contrast optical micrographs of PEH/PEB = 30/70 blend at room temperature after LLPS at 135 °C for different periods of time. Micrographs in Figure 4a,b show that the bicontinuous structures of the PEH/PEB = 30/70 blend can be observed, and they grow with time of LLPS. After LLPS at 135 °C for 12 h, the bicontinuous structures start to break up and two irregular phases appear. When the blend was cooled to room temperature, second-step phase separation in the already phase-separated domains happens and so does crystallization in both original PEH-rich and PEB-rich domains. The dark dots in the light (PEB-rich) domains should be the same as the dark parts in the PEH-rich domains. These dots are phase-separated PEH-rich domains after the second quench which should be similar to the continuous part of the PEH-rich domains after the second quench. This mechanism for the formation of dotlike structures can be illustrated schematically in Figure 1b. The newly formed small domains may reside in the originally larger domains, but sometimes they break up the boundaries of the larger ones. That is the reason why the phase boundaries in Figure 4a−c are much more jagged than they should be if the second-step phase separation and crystallization do not exist. When the domain sizes from the first phase separation become large enough, such as that in Figure 4d, the second-step phase separation within phase-separated domains can be observed clearly. However, because of the lower PEH concentration inside the PEB-rich domains, the PEB-rich domains were not broken up sufficiently to show the jagged edges.

Conclusions

The phase-separated structures developed via spinodal decomposition and double temperature quench in a blend of PEH and PEB were investigated with a combination of phase contrast optical microscope, polarized optical microscope, and atomic force microscope. The existence of fine structures within original PEB-rich domains has been observed, which is thought to be caused by the second-step phase separation. An additional phase separation occurs in the PEB-rich domains, in which this fine PEH-rich structure can further crystallize when the blend is cooled to room temperature. After the blend underwent LLPS for a long time, the higher branched PEH may concentrate in the PEB-rich domains due to relatively higher solubility with PEB and forms imperfect crystals. The observed morphology in the PEH/PEB blend consists of the phase-separated and crystallized small and fine domains within the large phase-separated domains.

Acknowledgment. The authors thank the financial support of KJCX2-SW-H107, 2003CB615600, 20490220, and "One Hundred Young Talents Program of Chinese Academy of Sciences".

Supporting Information Available: DSC thermograms of the PEH/PEB blends and neat PEH and PEB. This material is available free of charge via the Internet at http://pubs.acs.org.

References and Notes

(1) Balsara, N. P.; Fetters, L. J.; Hadjichristidis, N.; Lohse, D. J.; Han, C. C.; Graessley, W. W.; Krishnamoorti, R. *Macromolecules* **1992**, *25*, 6137.
(2) Lefebvre, A. A.; Lee, J. H.; Balsara, N. P.; Hammouda. B. *J. Chem. Phys.* **2002**, *116*, 4777.
(3) Sasaki, K.; Hashimoto, T. *Macromolecules* **1984**, *17*, 2818.
(4) Izumitani, T.; Hashimoto, T. *J. Chem. Phys.* **1985**, *83*, 3694.
(5) Hoffman, J. D.; Miller, R. L. *Macromolecules* **1988**, *21*, 3038.
(6) Lotz, B. *Eur. Phys. J. E* **2000**, *3*, 185.
(7) Wang, H.; Shimizu, K.; Kim, H.; Hobbie, E. K.; Wang, Z. G.; Han C. C. *J. Chem. Phys.* **2002**, *116*, 7311.
(8) Inaba, N.; Sato, K.; Suzuki, S.; Hashimoto, T. *Macromolecules* **1986**, *19*, 1690.
(9) Matsuba, G.; Shimizu, K.; Wang, H.; Wang, Z. G.; Han, C. C. *Polymer* **2003**, *44*, 7459.
(10) Tanaka, H.; Nishi, T. *Phys. Rev. Lett.* **1985**, *55*, 1102.
(11) Shimizu, K.; Wang, H.; Wang, Z.; Matsuba, G.; Kim, H.; Han, C. C. *Polymer* **2004**, *45*, 7061.
(12) Wang, Z.; Wang, H.; Shimizu, K.; Dong, J. Y.; Hsiao, B. S.; Han, C. C. *Polymer* **2005**, *46*, 2675.
(13) Zhang, X. H.; Wang, Z. G.; Muthukumar, M.; Han, C. C. *Macromol. Rapid Commun.* **2005**, *26*, 1285.
(14) Wang, H.; Shimizu, K.; Hobbie, E. K.; Wang, Z. G.; Meredith, J. C.; Karim, A.; Amis, E. J.; Hsiao, B. S.; Hsieh, E. T.; Han, C. C. *Macromolecules* **2002**, *35*, 1072.
(15) Gunton, J. D.; San Miguel, M.; Sahni, P. S. In *Phase Transitions and Critical Phenomena*; Domb, C., Lebowitz, J. L., Eds.; Academic Press: New York, 1983; p 269.
(16) Binder, K. In *Materials Science and Technology*; Haasen, P., Ed.; VCH: Weinheim, Germany, 1991; Vol. 5.
(17) Hashimoto, T. *Phase Transitions* **1988**, *12*, 47. Hashimoto, T. In *Materials Science and Technology*; Thomas, E. L., Ed.; VCH: Weinheim, Germany, 1993; Vol. 12.
(18) Hashimoto, T.; Itakura, M.; Hasegawa, H. *J. Chem. Phys.* **1986**, *85*, 6118.
(19) Okada, M.; Han, C. C. *J. Chem. Phys.* **1986**, *85*, 5317.
(20) Bates, F. S.; Wiltzius, P. *J. Chem. Phys.* **1989**, *91*, 3258.
(21) Jinnai, H.; Hasegawa, H.; Hashimoto, T.; Han, C. C. *Macromolecules* **1991**, *24*, 282.
(22) Schwahn, D.; Janssen, S.; Springer, T. *J. Chem. Phys.* **1992**, *97*, 8775.
(23) Hashimoto, T.; Jinnai, H.; Hasegawa, H.; Han, C. C. *Physica A* **1994**, *204*, 261.
(24) Ohnaga, T.; Inoue, T. *J. Polym. Sci., Part B: Polym. Phys.* **1989**, *27*, 1675.
(25) Okada, M.; Kwak, K. D.; Nose, T. *Polym. J.* **1992**, *24*, 215.
(26) Kwak, K. D.; Okada, M.; Chiba, T.; Nose, T. *Macromolecules* **1993**, *26*, 4047.
(27) Tao, J.; Okada, M.; Nose, T.; Chiba, T. *Polymer* **1995**, *36*, 3909.
(28) Tanaka, H. *Phys. Rev. E* **1995**, *51*, 1313.
(29) Cyganik, P.; Budkowski, A.; Raczkowska, J.; Postawa, Z. *Surf. Sci.* **2002**, *507*, 700.
(30) Sasha, Y. H.; Jones, R. A. L. *Nat. Mater.* **2005**, *4*, 782.
(31) Kwei, T. K.; Wang, T. T. In *Polymer Blends*; Paul, D. R., Ed.; Academic Press: New York, 1978; p178.
(32) Kamdar, A. R.; Hu, Y. S.; Ansems, P.; Chum, S. P.; Hiltner, A.; Baer, E. *Macromolecules* **2006**, *39*, 1496.
(33) We did the same experiments with other compositions of the blends, but this phenomenon is most obvious for the PEH/PEB = 30/70 sample. Therefore, we use this composition in the Results and Discussion section.
(34) Ribbe, A. E.; Hashimoto, T.; Jinnai, H. *J. Mater. Sci.* **1996**, *31*, 5837.
(35) Alamo, R. G.; Graessley, W. W.; Krishnamoorti, R.; Lohse, D. J.; Londono, J. D.; Mandelkern, L.; Stehling, F. C.; Wignall, G. D. *Macromolecules* **1997**, *30*, 561.
(36) Reichart, G. C.; Graessley, W. W.; Register, R. A.; Lohse, D. J. *Macromolecules* **1998**, *31*, 7886.
(37) Budkowski, A. *Adv. Polym. Sci.* **1999**, *148*, 1.
(38) Scheffold, F.; Eiser, E.; Budkowski, A.; Steiner, U.; Klein, J. *J. Chem. Phys.* **1996**, *104*, 8786.

MA061064I